

# Designing visual appearance using a structured surface

**Johansen, Villads Egede; Thamdrup, Lasse Højlund; Smitrup, Christian; Nielsen, Theodor; Sigmund, Ole; Vukusic, Peter**

*Published in:*
Optica

*Link to article, DOI:*
10.1364/OPTICA.2.000239

*Publication date:*
2015

*Document Version*
Publisher's PDF, also known as Version of record

Research Article Vol. 2, No. 3 / March 2015 / Optica 239


# Designing visual appearance using a structured surface

Villads Egede Johansen,[1,*] Lasse Højlund Thamdrup,[2] Kristian Smistrup,[2] Theodor Nielsen,[2] Ole Sigmund,[1] and Peter Vukusic[3]

[1]Technical University of Denmark, Department of Mechanical Engineering, 2800 Kgs. Lyngby, Denmark

[2]NIL Technology ApS, Diplomvej 381, 2800 Kgs. Lyngby, Denmark

[3]School of Physics, University of Exeter, Exeter EX4 4QL, UK

*Corresponding author: vejo@mek.dtu.dk

Received 9 October 2014; revised 20 January 2015; accepted 25 January 2015 (Doc. ID 224676); published 9 March 2015

**We present an approach for designing nanostructured surfaces with prescribed visual appearances, starting at design analysis and ending with a fabricated sample. The method is applied to a silicon wafer structured using deep ultraviolet lithography and dry etching and includes preliminary design followed by numerical and experimental verification. The approach comprises verifying all design and fabrication steps required to produce a desired appearance. We expect that the procedure in the future will yield structurally colored surfaces with appealing prescribed visual appearances.** 

***OCIS codes:*** (330.1690) Color; (050.1960) Diffraction theory; (240.6700) Surfaces; (290.0290) Scattering; (330.7326) Visual optics, modeling.

http://dx.doi.org/10.1364/OPTICA.2.000239

## 1. INTRODUCTION

Advances in nanotechnology are improving possibilities for designing structural colors. Recently, a range of techniques for creating synthetic structurally colored systems have been reported in the literature. The methods each utilize a very different production technique, ranging from self-assembly [1–4] to deposition, growth, embossing, and etching techniques [5–14]. The nanofabrication methods are often highly inventive with different limitations on geometries and materials and, thus, also on obtainable colors and angle dependence. The governing effects for color control are (layered) interference effects possibly combined with randomization [1,5,7–9,11,12,14], structural (particle) scattering [2–4,6], and surface plasmon effects [10,13]. The approaches mentioned—which by no means provide an exhaustive list—all have their limitations due to manufacturability, such as good color selectivity but little control of angular reflection, or expensive fabrication and/or design procedures. We therefore find that there is still room to discover methods that are reproducible on an industrial scale, cheap, applicable to different surface types and curvatures, and environmentally friendly, and exhibit controlled tunability.

Another important point is that all approaches considering surface coloration [1,3–6,8,10,13,14] except two [7,12] base their color selectivity and/or angular dependence on adding new materials to the surface. The two exceptions both have interference-like reflections, not smooth angular variations in color. Exploring the possibilities of surface manipulation techniques without addition of secondary materials to obtain a smooth, appealing color effect is one method to address many of the issues above.

In this paper we report results of our initial studies toward producing structural colors. We will address all the issues above, except tunability, by considering large batch manufacturable (preferably injection moldable) structured surfaces. The design freedom is currently limited by manufacturing constraints and tolerances for the choice of production processes. Despite this we are able to demonstrate here how to navigate the design and manufacturing process from specifications to a fabricated surface. We see this as a valuable step toward widespread use of structural color design in an industrial setting.

2334-2536/15/030239-07$15/0$15.00 

## 2. DESIGN APPROACH OUTLINE

The goal, when designing a system to exhibit structural colors, is to identify a structure with a desired visual response; see Fig. 1(a). The design of submicrometer features on a surface that extends millimeters or more is an overwhelming task. For this reason, if no systematic approach is used, the problem has to be divided into manageable components. An obvious choice that makes the computational task of predicting color reflection more accessible is to assume a form of structure that is repeated across the surface, such as is shown in Fig. 1(b). A regular structure with a fixed period is unfit for our purpose due to interference effects [15]. To avoid this we introduce height randomization in these repeated units [15,16]. The dominant effect of such an approach can be approximated analytically [15] and verified numerically before fabrication. This approach is represented in Fig. 1(c).

Using this technique means that the design challenge is broken down into two (decoupled) components: the design of a unit structure and the design of its randomization. In earlier works [15,17] we have shown how to design such unit structures for various 2D design goals, and we have also described how to incorporate the effect of randomization [15]. Production of such samples is challenging, and to test this approach a sample is fabricated using deep ultraviolet lithography (DUV) and dry etching. This will be described in Section 5. This means that only three levels of height can be used in designing the structure and its randomization, meaning that the final design will appear as shown in Fig. 1(d). A flow chart of this general design procedure applied to our study is depicted in Fig. 2.

The following four sections describe the individual design steps in Fig. 2.

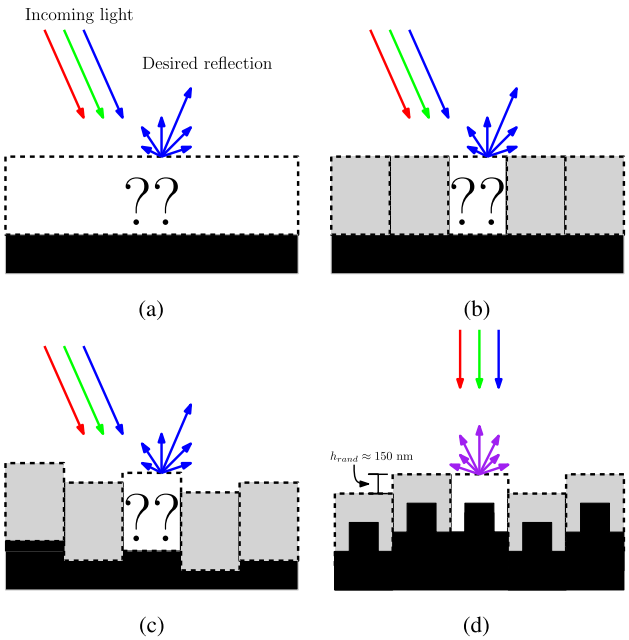


**Fig. 1.** (a) A general structural color problem: find a design that gives a prescribed reflection—e.g., a blue distribution—for incoming white light. (b) Due to many orders of magnitude difference in the analysis (ranging from a centimeter-sized surface to submicrometer electromagnetic waves) the analysis has to be divided into subparts, which is done here by assuming periodic repetition of the same structure. (c) Since a pure periodic structure gives rise to unwanted diffraction effects, this has to be avoided by also designing a way of "randomizing" the unit structure—here it is done by height translations. (d) To verify the approach in (a)–(c), a test structure is produced to see how measurements fit analysis.

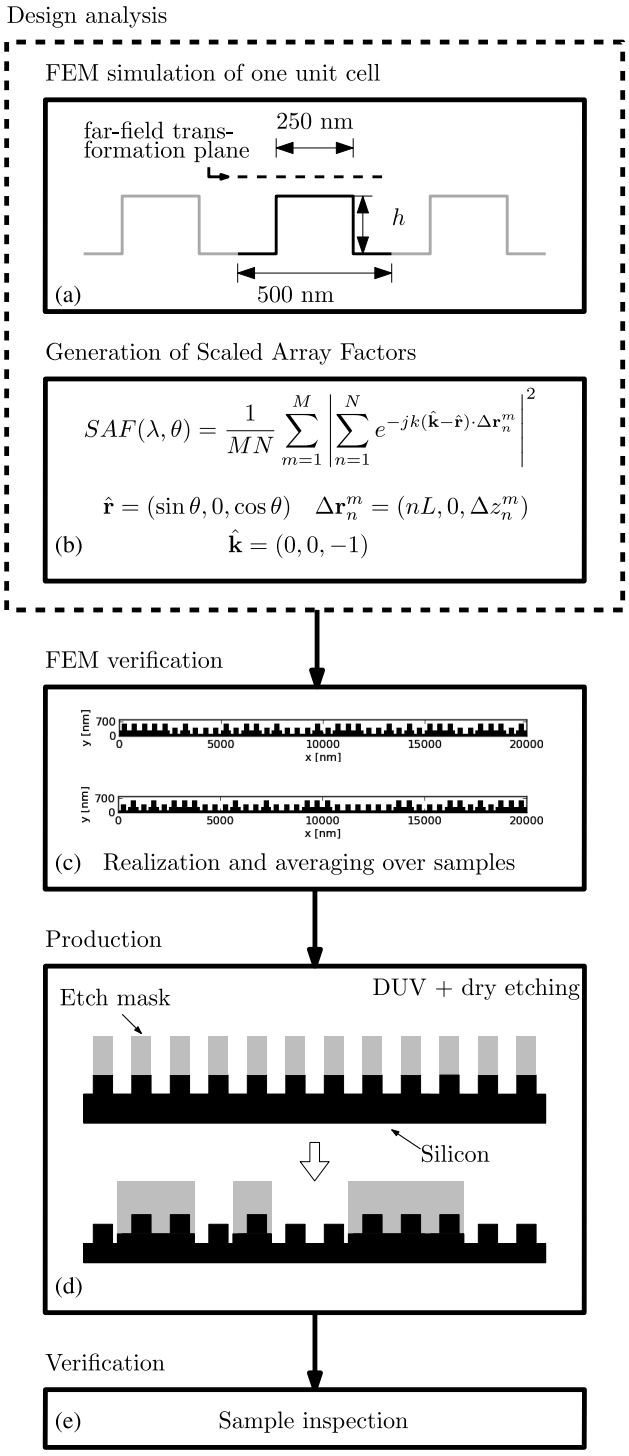


**Fig. 2.** Design workflow used to create a structurally colored surface—in this case by using DUV and dry etching. (a) First a unit structure is defined and analyzed, while (b) at the same time the effect of the scaled array factor (SAF) is calculated and taken into account. (c) This design is then verified using a full FEM model, (d) which then gives the dimensions from which to produce a sample. (e) Last, the result is verified.

## 3. STEP 1: STRUCTURE DESIGN

Our previous works [15,17–19] focused on how to model and design dielectric structures for prescribed color responses in a systematic way. In this paper we focus on the sample production and verification steps and have therefore chosen to use a 50% duty cycle (half-pitch) line grating with a height of 215 nm as the unit structure for our structurally colored surface. This structure can be produced using traditional methods and equipment at our disposal. The choice of height gives several distinct specular reflection peaks and dips in the visible spectrum. In particular, simulations will show that both a strong dip and peak exist below a wavelength of 500 nm, thus making it possible to investigate how well energy either can be kept in—or transferred from—specular reflection due to overlaid randomization. Since line gratings are invariant in depth, it means that if we chose a randomization with the same invariance properties, the reflection of light will be confined to a plane, making experimental measurements more straightforward. A duty cycle of 50% also gives the largest color contrast with respect to specular reflection {[19], Fig. 7(a)}. A binary random pattern with a height of 150 nm is chosen for the randomization, which maximizes scattering around 600 nm [15].

The unit structure period is chosen to be 500 nm so that shorter visible wavelengths will diffract and larger visible wavelengths will not, for normal incidence. This makes it possible to capture different types of behavior in one measurement at normal incidence. It also complies with the choice of line grating height, since light from the strong dip and peak will be diffracted.

To predict the reflection, a one unit structure was simulated for unpolarized light (power average of $E_z$, $H_z$) using the finite-element-method (FEM) with periodic boundary conditions as described in earlier work [17], and afterward postprocessed by incorporating the random effect as described in [19]. The optical properties of silicon were taken from the literature [20]. This means that the scattered unit far-field radiance $L_u$ was calculated first and was subsequently multiplied by what we called the scaled array factor (SAF) [19]. The total radiance $L$ can be described as

$$L = L_u \underbrace{\frac{1}{M}\sum_{m=1}^{M}\left|\frac{1}{N}\sum_{n=1}^{N} e^{-ik(n\ell_x \sin\theta + \Delta z_n^m(\cos\theta+1))}\right|^2}_{\text{SAF}}, \quad (1)$$

where $\theta$ is the reflection angle, $i$ is the imaginary unit, $\ell_x$ is the length of one period, $\Delta z_n^m$ is a uniform random number taking on either 0 or 150 nm, and $N$ and $M$ are loosely connected to the coherence of the incoming light [16,19]. The resulting reflection of the unit structure is shown in Fig. 6(a) and the SAF is shown in Fig. 6(b). By multiplying the results they produce the total radiance shown in Fig. 6(c).

## 4. STEP 2: DESIGN VERIFICATION

The approximation described in Step 1 provides an efficient route for analysis, which is often needed in the design phase. To verify the approximation of the final design, full FEM simulations were used (with the same number of averages and choices of $\Delta z_n^m$). The result is presented in Fig. 6(d) and takes several days to generate on an eight core machine, since each model contains $5 \cdot 10^5$ elements and an average of approximately $M = 100$ models is needed for a meaningful response. This is why a full simulation is not feasible for the design phase.

The overall behavior is seen to be similar to the behavior of the approximate model. The most notable differences are that the very low intensity areas and reflection minima are less pronounced, the peak intensities are in general lower, and the first-order diffraction modes seems to have shifted in intensity. We expect even better fits for structures with smoother angular reflection spectra.

## 5. STEP 3: SAMPLE PRODUCTION

The sample was produced on a single-side-polished 100 mm diameter silicon wafer with a thickness of 525 μm. A sketch of the process steps is presented in Fig. 2(d). The optimal DUV dose for the resist (JSR-M230Y from JSR Micro, 350 nm thickness) exposure of the underlying periodic grating was found to be 220 J/m$^2$ to ensure a 50% duty cycle after pattern transfer into silicon by advanced silicon etching (STS MESC Multiplex ICP Advanced Silicon Etcher). The second DUV exposure was performed in JSR-M35G resist (from JSR Micro), thickness 750 nm, at a DUV dose of 320 J/m$^2$ to ensure complete coverage of the periodic grating. The design of the DUV reticle did not incorporate dose compensation, so we aimed for maximum pattern replication fidelity of structures with the smallest line width (i.e., 500 nm). The dry etching of the random grating was performed using an inductive coupled plasma etch (SPTS ICP Metal Etcher) to ensure high precision in the etch depth. Afterward the sample wafer was cleaned using oxygen plasma and Piranha solution.

## 6. STEP 4: SAMPLE VERIFICATION

### A. Geometry Inspection

The geometry of the produced sample was inspected using scanning electron microscopy (SEM) and atomic force microscopy (AFM). A selection of SEM images is presented in Fig. 3: Fig. 3(a) shows one corner of the sample, and it is possible to see the misalignment between the two reticles that were used. The misalignment is almost purely translational, with less than $10^{-3}$ degrees of rotation with respect to each other. This means that the two patterns are experiencing a shift of around 50 nm per centimeter. Since our samples are 1 cm × 1 cm, no gradual color change was observed due to this effect. Misalignment is expected to affect reflection properties for this test geometry over larger areas. See Media 1 for a representation of the effect of misalignment. At the same time we do not believe that the effect will be observable under normal lighting conditions—in particular for a geometry optimized for an appealing color effect, where the randomization will be in 2D [5]. Figure 3(b) shows that the period of the grating is approximately 505 nm, and the trenches are measured to be around 243 nm. Figure 3(b) also shows that the difference between the trenches that have been

etched farther down by the randomization process and those that have not, is small. Figure 3(c) shows a more distinct

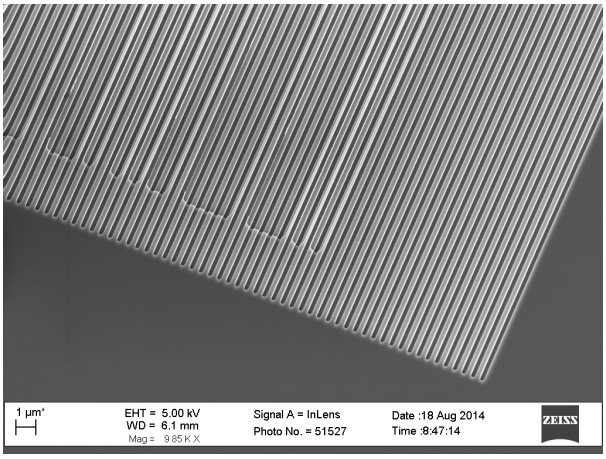


(a)

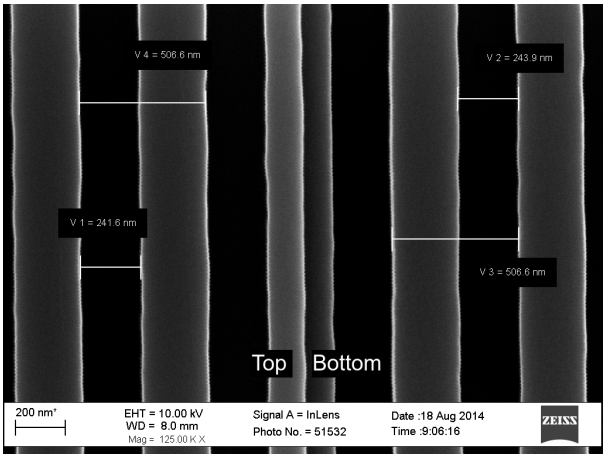


(b)

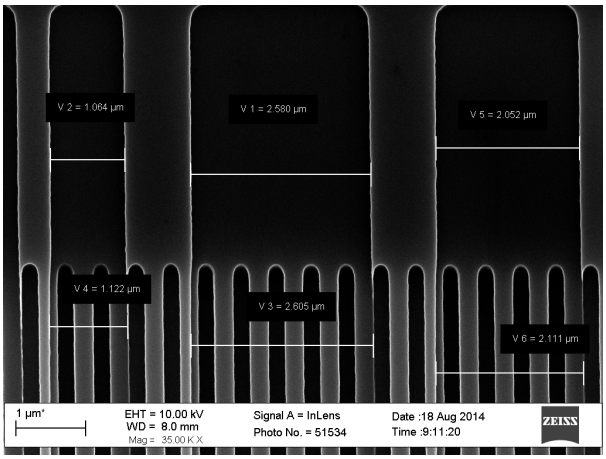


(c)

**Fig. 3.** SEM images of the produced structural color sample. (a) The structure overview shows the unit half-pitch grating with the random grating visible inside the half-pitch grating as undulations to the otherwise regular pattern. (b) Close-up of the unit grating structure at the edge of the random structure showing a step height change. The lateral dimensions of the unit grating does not change between steps. (c) Close-up of the random grating. The random grating is indeed random in its lateral dimension.

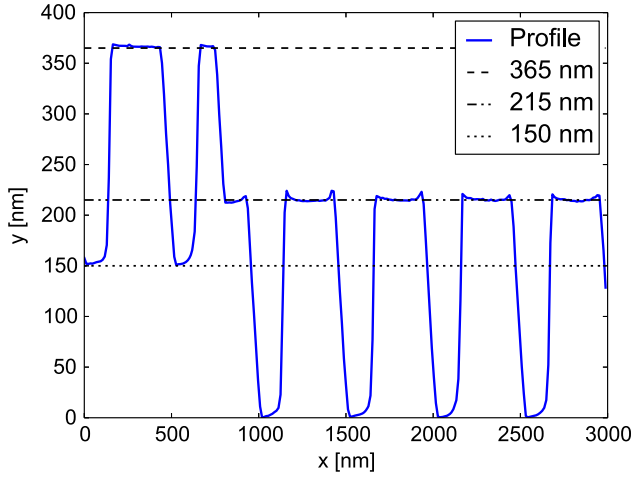


**Fig. 4.** Surface profile of the silicon structure extracted from AFM measurements.

difference from the predicted design, namely, the width of the trenches of the random overlay has been etched wider than planned (~30 nm on each side in the area without the underlying grating). These trenches can also be seen to widen even further when etched on top of the line grating (up to ~60 nm on each side). Since the nonetched parts are smaller, the repetition length of the randomization unit is maintained.

The surface profile of the structure is shown in Fig. 4. From several images similar to this, we conclude that the underlying periodic line grating had been etched 215 nm into the Si substrate, and that performing the extra etching of the randomization reticle only slightly influences the line grating heights. The etch depth of the random grating is approximately 150 nm.

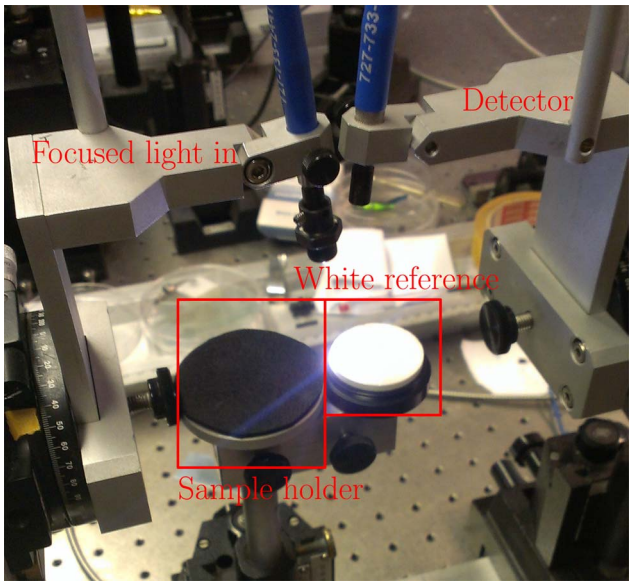


**Fig. 5.** Setup for reflectance characterization of the produced sample. The sample (or calibration reference) is lit by a focused white-light source from a 1000 µm fiber and collected by a 200 µm fiber connected to a USB2000 Ocean Optics spectrometer.

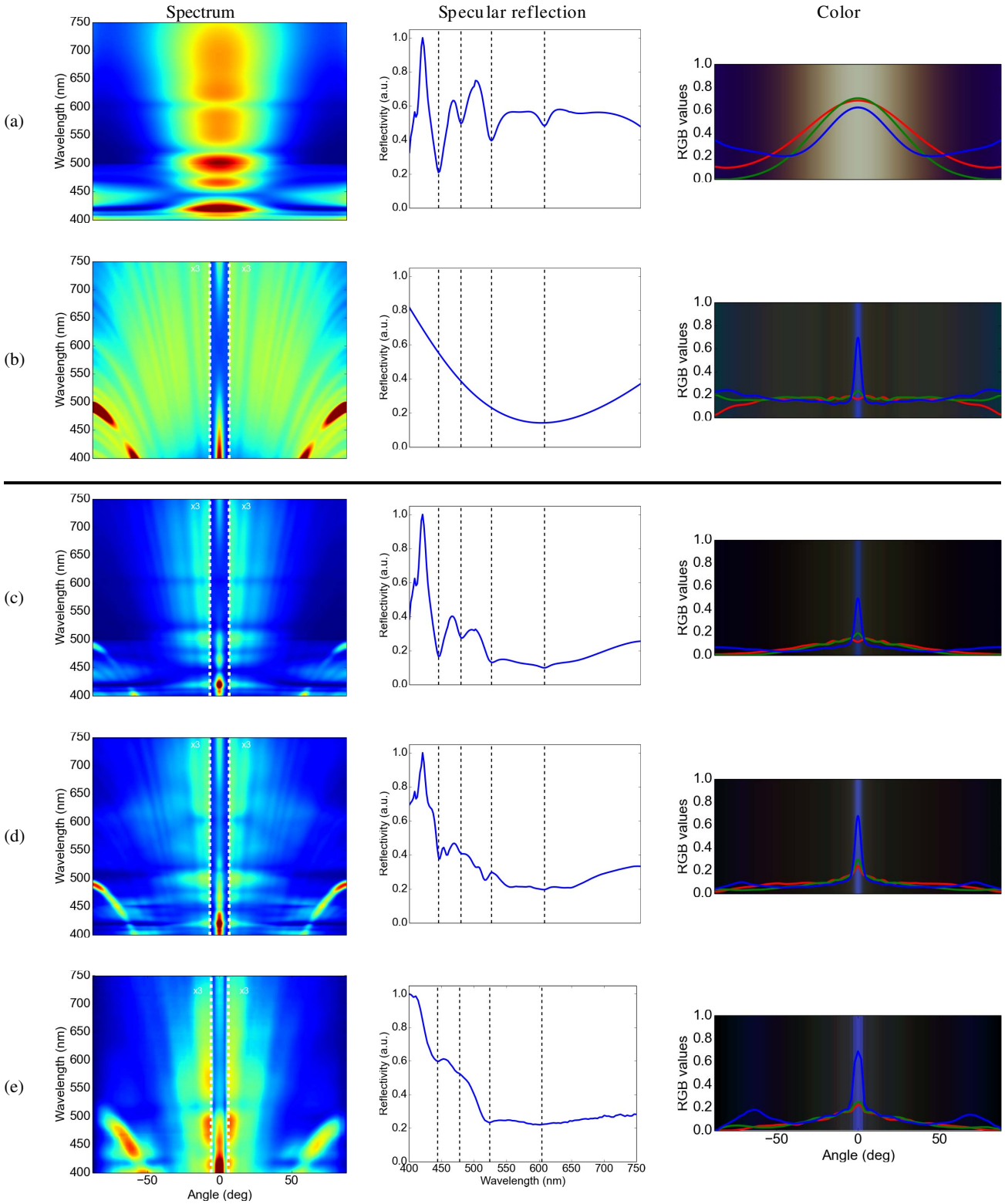


**Fig. 6.** Results of each design step in obtaining a structurally colored surface: (a) the response of the chosen unit structure and (b) the influence of randomization (SAF). (c) The product of these two then yields an approximate response. (d) A full wave FEM simulation verifies the result before production, and (e) measurements on a produced sample are compared with the predicted result. All spectra are given in radiance (which here means intensity divided by cosine to the angle of reflection). All simulated data has been Gaussian blurred using an image filter as a simple way of incorporating the effect of the finite-sized detector in the measurement setup. Note that some values in the contour plot are cropped in order to get a better color representation.

### B. Optical Verification

The sample reflectance was characterized by focusing an unpolarized white-light source through a fiber almost normal to its surface (tilted only enough to avoid incident light being reflected back into the source) and then scanning a 200 μm optical fiber in the plane of reflection; see Fig. 5. The method used is described in detail elsewhere [21].

The small deviation from normal incidence means that the reflection plane due to invariance is slightly curved [22], but by visual inspection it was confirmed that the reflection plane was covered by the detecting fiber. It might have contributed to a decrease in intensity for larger angles. The result of the measurement is presented in Fig. 6(e). The angular resolution when recording the measurements was 2 deg, and the spectral resolution was better than 0.5 nm. For large angles, the received intensity was low, and the signal-to-noise ratio therefore worse than for small angles.

## 7. RESULTS ANALYSIS

Many of the observed features on the contour plots in Fig. 6 can be described from the combination of the unit structure and the SAF approximation—that is, either they come from the choice of unit structure or choice of randomization. Figure 7 shows an annotated version of the FEM response and this can be used to provide further understanding on how to interpret the observed reflection data. First of all, it is noticed how the decrease in specular intensity around 450 nm is due to the choice of unit structure [see Figs. 6(a) and 7], whereas the specular roll-off at longer wavelength is caused by the SAF [see Fig. 6(b)]. In the first-order grating mode, we see several intensity dips, which all can be ascribed either to unit structure or SAF (see Fig. 7). Another set of distinct features in the numerical verification is the group of lines that correspond to higher order grating modes (multiples of 500 nm). These are caused by the randomization pattern [Figs. 7 and 6(b)] and will be referred to as superperiod modes in the rest of this text. These superperiods are better quenched in the approximation than the verification. This is probably due to the periodic boundary conditions assumed when simulating one unit compared to the disturbed periodicity in the full simulation, making the destructive interference condition less ideal. A final important feature is the control of intensity distribution, which to a large extent is mediated by the unit cell structure [Figs. 6(a) and 7]. This arises because there is a weak wavelength dependence for the spread in intensity of the SAF at longer wavelengths [Fig. 6(b)].

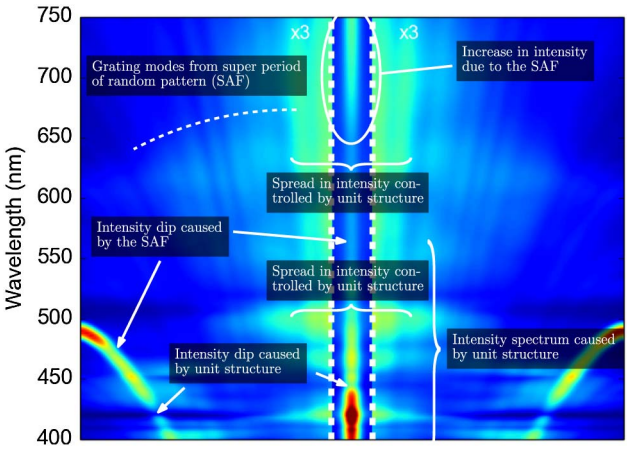


**Fig. 7.** An annotated version of the numerical verification presented in Fig. 6(d) explaining where the effects visible on the plot originate from.

Comparing the measurement results in Fig. 6(e) and Figs. 6(c) and 6(d), we see that a fit between experimental data from the fabricated sample and reflection data arising from the FEM model is generally very good. We notice several features indicating this fit. First, the grating modes from superperiods are still visible, albeit at much lower intensity; this is probably due to the general smoothing effect observed in the measurements. Second, the spectral intensity profile of the first-order grating mode is similar to that observed in the model. Some features indicating a clear difference between experimental data and the model are also present: the broad scattering around the specular direction for larger wavelengths is much less pronounced in the experimental data; the amount of scattered intensity around the specular direction for lower wavelengths is much more pronounced in the experimental data than in the model. Since the sample geometry is of high precision, we believe that the difference between model and measurements is caused primarily by nanometer-sized height variations in the sample. This decreases the flawless interference effects present in the simulation. This can also explain why, for example, the intensity minima in specular reflection are much less pronounced in the model compared to the measurements.

## 8. CONCLUSIONS

We have presented a method for fabricating surface structures that leads to a target structural color performance. The methods consist of several steps: a unit design phase, a randomization design phase, verification, and production. This enables the fabrication of a structurally colored surface by the workflow shown in Fig. 2. Despite some open questions, a general match between modeling and experiment was observed, verifying the overall design approach. In earlier work some of the design steps have been discussed in detail [15,17,19], and this should enable more advanced designs featuring more complex and appealing visual appearances. In the future these would be based on more complex structures—especially by extending the approach to 3D.

We believe that this approach makes it possible to explore the design space for different manufacturing technologies and materials. A long-term goal is to be able to create cheap, mass-manufacturable, environmentally friendly structurally colored surfaces based on polymer materials and mass-production techniques like hot embossing and injection molding. The low refractive index of these materials might limit total reflection compared to silicon but the technology is still relevant for applications like text, color symbols, security logos, and decorative purposes.

## FUNDING INFORMATION

USAF (FA9550-10-1-002); Innovation Fund Denmark (ODAAS and NanoPlast).

## ACKNOWLEDGMENT

The authors would like to thank Mark Heath and David Hudson of the Centre for Graphene Science, University of Exeter, for help on sample preparation. Also Lesley Wears of College of Engineering, University of Exeter, is thanked for help on characterization. Financial support from the U.S. Air Force Office, award number FA9550-10-1-0020, is gratefully acknowledged.

## REFERENCES

1. M. Kolle, P. M. Salgard-Cunha, M. R. J. Scherer, F. Huang, P. Vukusic, S. Mahajan, J. J. Baumberg, and U. Steiner, "Mimicking the colourful wing scale structure of the *Papilio blumei* butterfly," Nat. Nanotechnol. **5**, 511–515 (2010).
2. C. I. Aguirre, E. Reguera, and A. Stein, "Colloidal photonic crystal pigments with low angle dependence," Appl. Mater. Interfaces **2**, 3257–3262 (2010).
3. C. E. Finlayson and J. J. Baumberg, "Polymer opals as novel photonic materials," Polym. Int. **62**, 1403–1407 (2013).
4. N. Koay, I. B. Burgess, T. M. Kay, B. A. Nerger, M. Miles-Rossouw, T. Shirman, T. L. Vu, G. England, K. R. Phillips, S. Utech, N. Vogel, M. Kolle, and J. Aizenberg, "Hierarchical structural control of visual properties in self-assembled photonic-plasmonic pigments," Opt. Express **22**, 27750–27768 (2014).
5. A. Saito, Y. Miyamura, Y. Ishikawa, J. Murase, M. Akai-Kasaya, and Y. Kuwahara, "Reproduction, mass-production, and control of the *Morpho*-butterfly's blue," Proc. SPIE **7205**, 720506 (2009).
6. J. Yip, S.-P. Ng, and K.-H. Wong, "Brilliant whiteness surfaces from electrospun nanofiber webs," Text. Res. J. **79**, 771–779 (2009).
7. L. Yisen, C. Yi, L. Zhiyuan, H. Xing, and L. Yi, "Structural coloring of aluminum," Electrochem. Commun. **13**, 1336–1339 (2011).
8. M. A. Kats, R. Blanchard, P. Genevet, and F. Capasso, "Nanometre optical coatings based on strong interference effects in highly absorbing media," Nat. Mater. **12**, 20–24 (2012).
9. M. Aryal, D.-H. Ko, J. R. Tumbleston, A. Gadisa, E. T. Samulski, and R. Lopez, "Large area nanofabrication of butterfly wing's three dimensional ultrastructures," J. Vac. Sci. Technol. B **30**, 061802 (2012).
10. K. Kumar, H. Duan, R. S. Hedge, S. C. W. Koh, J. N. Wei, and J. K. W. Yang, "Printing colour at the optical diffraction limit," Nat. Nanotechnol. **7**, 557–561 (2012).
11. M. Kolle, A. Lethbridge, M. Kreysing, J. J. Baumberg, J. Aizenberg, and P. Vukusic, "Bio-inspired band-gap tunable elastic optical multilayer fibers," Adv. Mater. **25**, 2239–2245 (2013).
12. Y. Chuo, C. Landrock, B. Omrane, D. Hohertz, S. V. Grayli, K. Kavanagh, and B. Kaminska, "Rapid fabrication of nano-structured quartz stamps," Nanotechnology **24**, 055304 (2013).
13. J. S. Clausen, E. Højlund-Nielsen, A. B. Christiansen, S. Yazdi, M. Grajower, H. Taha, U. Levy, A. Kristensen, and N. A. Mortensen, "Plasmonic metasurfaces for coloration of plastic consumer products," Nano Lett. **14**, 4499–4504 (2014).
14. N. Schneider, C. Zeiger, A. Kolew, M. Schneider, J. Leuthold, H. Hölscher, and M. Worgull, "Nanothermoforming of hierarchical optical components utilizing shape memory polymers as active molds," Opt. Mater. Express **4**, 1895–1902 (2014).
15. V. E. Johansen, "Optical role of randomness for structured surfaces," Appl. Opt. **53**, 2405–2415 (2014).
16. A. Saito, M. Yonezawa, J. Murase, S. Juodkazis, V. Mizeikis, M. Akai-Kasaya, and Y. Kuwahara, "Numerical analysis on the optical role of nano-randomness on the *Morpho* butterfly's scale," J. Nanosci. Nanotechnol. **11**, 2785–2792 (2011).
17. J. Andkjær, V. E. Johansen, K. S. Friis, and O. Sigmund, "Inverse design of nanostructured surfaces for color effects," J. Opt. Soc. Am. B **31**, 164–174 (2014).
18. K. S. Friis and O. Sigmund, "Robust topology design of periodic grating surfaces," J. Opt. Soc. Am. B **29**, 2935–2943 (2012).
19. V. E. Johansen, J. Andkjær, and O. Sigmund, "Design of structurally colored surfaces based on scalar diffraction theory," J. Opt. Soc. Am. B **31**, 207–217 (2014).
20. E. D. Palik, *Handbook of Optical Constants of Solids* (Academic, 1997).
21. P. Vukusic and D. G. Stavenga, "Physical methods for investigating structural colours in biological systems," J. R. Soc. Interface **6**, S133–S148 (2009).
22. J. E. Harvey and C. L. Vernold, "Transfer function characterization of scattering surfaces: Revisited," Proc. SPIE **3141**, 113–127 (1997).